Proc. Natl. Acad. Sci. USA
Vol. 95, pp. 1242–1246, February 1998
Neurobiology

Changes in cell-cycle kinetics during the development and evolution of primate neocortex

DAVID R. KORNACK* AND PASKO RAKIC

Section of Neurobiology, Yale University School of Medicine, New Haven, CT 06510

Contributed by Pasko Rakic, December 4, 1997

ABSTRACT **The evolutionary expansion of neocortical size in mammals is particularly prominent in anthropoid primates (i.e., monkeys, apes, and humans) and reflects an increased number of cortical cells, yet the developmental basis for this increase remains undefined. Cortical cell production depends on the length of the cell-division cycle of progenitor cells during neurogenesis, which previously has been measured only in smaller-brained rodents. To investigate whether cortical expansion in primates reflects modification of cell-cycle kinetics, we determined cell-cycle length during neurogenesis in the proliferative cerebral ventricular zone of fetal rhesus monkeys, by using cumulative S-phase labeling with bromodeoxyuridine. Cell-cycle durations in monkeys were as much as 5 times longer than those reported in rodents. Nonetheless, substantially more total rounds of cell division elapsed during the prolonged neurogenetic period of the monkey cortex, providing a basis for increased cell production. Moreover, unlike the progressive slowing that occurs during cortical development in rodents, cell division accelerated during neurogenesis of the enlarged cortical layers in monkeys. These findings suggest that evolutionary modification of the duration and number of progenitor cell divisions contributed to both the expansion and laminar elaboration of the primate neocortex.**

A hallmark of brain evolution is the enlargement of the mammalian neocortex. This enlargement is unusually prominent in anthropoid primates (i.e., monkeys, apes, and humans) (1), and is apparently associated with the specialized perceptual, cognitive, and social adaptations that characterize this group (2–5). While this enlargement reflects an increased number of cortical cells (6), the developmental basis for this increase remains undefined.

In mammals, including primates, neocortical neurons are generated during a restricted period of early ontogeny from the cerebral ventricular zone (VZ), a primitive epithelial sheet of dividing neural progenitor cells lining the cerebral ventricles. After their final division, postmitotic neurons migrate outward from the VZ and settle in an orderly, inside-out sequence, forming concentric layers (designated VI through II) in the cortical plate, the early-born cells constituting the deep layers and successively later-born cells forming progressively more superficial layers (7–10).

The increased number of cells in the enlarged primate neocortex presumably reflects evolutionary modifications in the neurogenetic program, resulting in greater cell production. Accordingly, a comparison of cell-proliferation parameters between anthropoid primates and mammals that have smaller neocortices could reveal the specific nature of such modifications. A critical determinant of cortical cell production is the duration of the cell-division cycle, which defines the number of successive cell divisions that elapse during the neurogenetic period. Cell-cycle duration has been well documented in studies of neocortical development in rodents, in which successive cell cycles progressively lengthen from 8 (mice) or 11 hr (rats) to almost 20 hr over a week-long neurogenetic period (11–15). However, the length of the cell cycle has not been defined during cortical development in any primate species, leaving fundamental questions of neocortical development and evolution unanswered. Are the cell cycle durations that have been measured in the small, rapidly developing rodent neocortex conserved in a primate with a 100-fold larger neocortex (16) and 10-fold longer neurogenetic period (8)? Alternatively, is the cell cycle in primates modified to scale proportionately with their prolonged neurogenetic period, such that the total number of successive cell divisions in the neurogenetic period is conserved across species?

To address these issues, we determined the length of both the cell cycle (Tc) and its DNA-synthetic (S) phase (Ts) in the VZ of the rhesus monkey, a nonhuman anthropoid primate, at embryonic day (E) 40, E60, and E80, corresponding to the beginning of the first, middle, and last third of the 60-day cortical neurogenetic period, respectively (8). Tc and Ts were estimated by cumulatively labeling progenitor cells in the VZ with bromodeoxyuridine (BrdUrd), a thymidine analog that is incorporated into replicating DNA during S phase (17). For analysis, we chose the VZ of the medial occipital wall, which generates the neurons of the prospective primary visual cortex (18). The timetable of neurogenesis for this cortical region is known (8), as is the number of neurons in each layer in the adult monkey (19). Accordingly, analysis of this region provided an opportunity to correlate cell cycle kinetics at a given stage of neurogenesis with the timing of the generation and eventual allocation of neurons to particular cortical layers.

MATERIALS AND METHODS

BrdUrd Injections. All animal care and experimentation were conducted in accordance with institutional guidelines. For timed pregnancies, female rhesus monkeys (*Macaca mulatta*) were caged with males for 3 days; the middle day was designated as the day of conception (E1). By this method, the estimated age of a monkey fetus has a maximal variation of ±1 day in its 165-day gestation. Twelve pregnant monkeys with fetuses at E40, E60, or E80 were anesthetized and injected intravenously with BrdUrd (Sigma; dissolved in saline with 0.007 M NaOH). For each fetal age, two pregnant monkeys each received a single injection of BrdUrd and another two pregnant monkeys each received two successive injections spaced 2 hr apart to cumulatively label progenitor cells that enter S phase during a 2-hr period. Each injection was a

The publication costs of this article were defrayed in part by page charge payment. This article must therefore be hereby marked "*advertisement*" in accordance with 18 U.S.C. §1734 solely to indicate this fact.

Abbreviations: VZ, ventricular zone; E*n*, embryonic day *n*; Tc, length of the cell cycle; Ts, length of the S phase of the cell cycle; BrdUrd, 5-bromodeoxyuridine; LI, labeling index.

*To whom reprint requests should be addressed at: Section of Neurobiology, Yale University School of Medicine, 333 Cedar Street, Room C-303, New Haven, CT 06510. e-mail: kornack@biomed.med.yale.edu.

constant dose of 50 mg of BrdUrd per kg of body weight. Thirty minutes after administration of either the single or the second injection, accordingly, fetuses were delivered by cesarean section and brains were immediately harvested and processed for BrdUrd immunohistochemistry. Injections and surgeries were performed between 9:00 a.m. and noon, as was done in previous rodent studies (11, 15), to control for potential circadian effects on cell-cycle kinetics (20). Each fetus was from a different pregnant monkey.

Tissue Processing and BrdUrd Immunohistochemistry. Brains of E60 and E80 fetuses were immediately removed and fixed overnight in 70% (vol/vol) ethanol at 4°C. Brains were dehydrated in graded alcohol solutions, cleared in xylene, embedded in paraffin, and serially sectioned at 8 μm in the coronal plane. For E40 embryos, the entire head was processed. Sections were mounted on glass slides and processed for BrdUrd immunohistochemistry as described previously (17, 21). Briefly, sections were immersed in 2 M HCl for 1 hr and were stained for BrdUrd by using mouse anti-BrdUrd monoclonal antibodies (Becton Dickinson; 1:75), biotinylated horse anti-mouse IgG (Vector Laboratories, 1:200), the Vector ABC Elite kit, and diaminobenzidine with 0.02% cobalt chloride and 0.02% nickel ammonium sulfate for color intensification. Sections were counterstained with 0.1% aqueous basic fuchsin.

Calculation of Tc and Ts. For analysis, BrdUrd-labeled and -unlabeled cell nuclei were scored within a demarcated sector of VZ in the medial occipital wall, using a calibrated computerized counting system. In the E40 brains, the occipital region was designated as the posterior-most one-fifth of the cerebrum, whereas at E60 and E80 the medial occipital wall was indicated by the incipient calcarine sulcus. The counting sector in E40 and E60 brains was 138 μm long, with the ventricular surface at its base. In E80 brains, the sector was extended to 240 μm, to compensate and ensure an adequate sample size for the thinner VZ at this age. Cells within a sector were counted throughout the entire radial thickness of the VZ, from the ventricular surface to either the primitive plexiform layer (at E40) or the subventricular zone (at E60 and E80). The VZ was distinguishable from the subventricular zone on the basis of the shape, orientation, and packing density of constituent cell nuclei, and the presence of abventricular mitotic figures seen only in the latter (13). Endothelial cells were not counted, and neuroepithelial nuclei lying on the lateral but not the medial border of the sector were counted. For each brain, an average labeling index (LI), which is the proportion of labeled cells to total (labeled plus unlabeled) cells, was determined by averaging the LIs of four nonadjacent sections within a consecutive series of seven to nine sections. More than 4,000 total nuclei were counted in E40 brains, 8,500 nuclei in E60 brains, and 5,000 nuclei in E80 brains.

To calculate Tc and Ts, the mean LI of each brain was plotted as a function of time after initial BrdUrd injection (Fig. 2). Using a linear regression analysis, a least-squares line was best-fit to the four data points for each age (i.e., two LIs at t = 0.5 hr and two LIs at t = 2.5 hr). The slope of the line is a measure of the additional proportion of cells that entered S phase during the 2-hr interval between injections, and thus indicates the rate of the cell division cycle (i.e., 1/Tc) (17). Ts was derived from the value (Ts/Tc)·GF, which is the extrapolated y intercept of the slope (17) and in which the growth fraction (GF) is unity (see below).

We used an abridged version of the cumulative labeling method previously used to measure Tc and Ts in rodents. In these studies, additional fetuses, receiving progressively greater numbers of injections of label at 2- to 3-hr intervals for a time period of $\geq$(Tc − Ts), were used to extend the cumulative labeling slopes to the point at which the total proliferative population is saturated with label (i.e., when the maximal LI is achieved) (14, 17, 22). Such saturation slopes allow the determination of the GF (i.e., that fraction of the cell population that is proliferating) and the shape of the least-squares slope best fit to the data points. Complete saturation slopes were not feasible to obtain in monkeys because of restricted availability of the required additional fetuses and prohibitive difficulties associated with providing a continuous BrdUrd infusion intravenously to additional pregnant monkeys for 18- to 40-hr periods. Therefore, in calculating values of Tc and Ts from our LI slopes, we assumed, on the basis of the previous rodent results, that the GF of monkey VZ cell population is virtually 100%, as it is in rats (14) and mice (12, 15). (Note that a GF even as low as 90% would decrease the Tc values we obtained by only 10%.) We also assumed that BrdUrd accumulation to saturation in the monkey VZ is linear, as demonstrated in rodents (22, 23); therefore, estimating Tc and Ts from a linear slope best-fit to data from two survival times (i.e., 0.5 and 2.5 hr) in monkeys is reasonable.

RESULTS

Appearance of the Monkey VZ. We compared the appearance of the fetal VZ in monkeys to that previously described in studies of cortical neurogenesis in rodents (15, 22, 24, 25). In monkeys as in mice, 30 min after a single BrdUrd injection, most BrdUrd-labeled cell nuclei were concentrated in the outer half to two-thirds of the VZ, whereas mitotic (M-phase) figures were confined to the ventricular surface (Fig. 1). This pattern reflects the systematic "to-and-fro" movement of progenitor cell nuclei within the VZ as they transit the successive phases of the cell cycle (i.e., G_1, S, G_2 and M) (22, 24). Between E40 and E60 the thickness of the VZ in monkeys increased because of a radial increase in the number of progenitor cells (Fig. 1). Subsequently, by E80 the VZ had drastically thinned to measure only a few nuclei across. Similar expansion and reduction of the VZ over the cortical neurogenetic period also occur in rats and mice (15, 25). Thus, with regard to the distribution of BrdUrd labeling and the developmental profile of VZ thickness during neurogenesis, the monkey VZ appeared similar to that in rodents.

Developmental Changes in Cell Cycle Length. We analyzed cumulative LIs (Fig. 2) to obtain estimates of cell-cycle and S-phase durations for the monkey VZ cell population. At the onset of cortical neurogenesis (E40) the cell cycle was 22.7 hr long (Fig. 3). By E60, as neurogenesis of layer VI is ending and layer V is beginning (8), the cycle had lengthened to 54.1 hr. By E80, as neurogenesis of layer IV finishes and layer III begins, the cell cycle had shortened to 27.4 hr. Compared with values for Tc in rodents, these estimates in monkeys are approximately 2 to 5 times longer, depending on the corresponding stage of cortical neurogenesis [e.g., in mice at E11, E13, and E15, Tc is 8.1 hr, 11.4 hr, and 17.5 hr, respectively (15)] (Fig. 4*A*). Further, the shortening of the cell cycle during cortical layer IV neurogenesis in monkeys contrasts strikingly with the gradual lengthening of the cell cycle described in rodents (11, 15) (Fig. 4*A*). This finding indicates that the continuous lengthening of the cell cycle during neurogenesis reported in rodents is not a universal feature of mammalian cortical development. Thus, whereas the monkey VZ appears similar histologically to that of rodents, dynamically it differs in both the duration and developmental course of the cell cycle.

Duration of S Phase. Because the cell cycle is the sum of its component phases, its prolongation in monkeys compared with rodents could be due to species differences in the duration of one or more particular phases. To understand the basis for the prolonged cell cycles in the monkey VZ, we examined the length of S phase during cortical neurogenesis and compared the values with estimates reported in similar cumulative labeling studies in rodents. Our analysis indicated that Ts in monkeys was 5.2 hr at E40, lengthened to 14.9 hr by E60, then

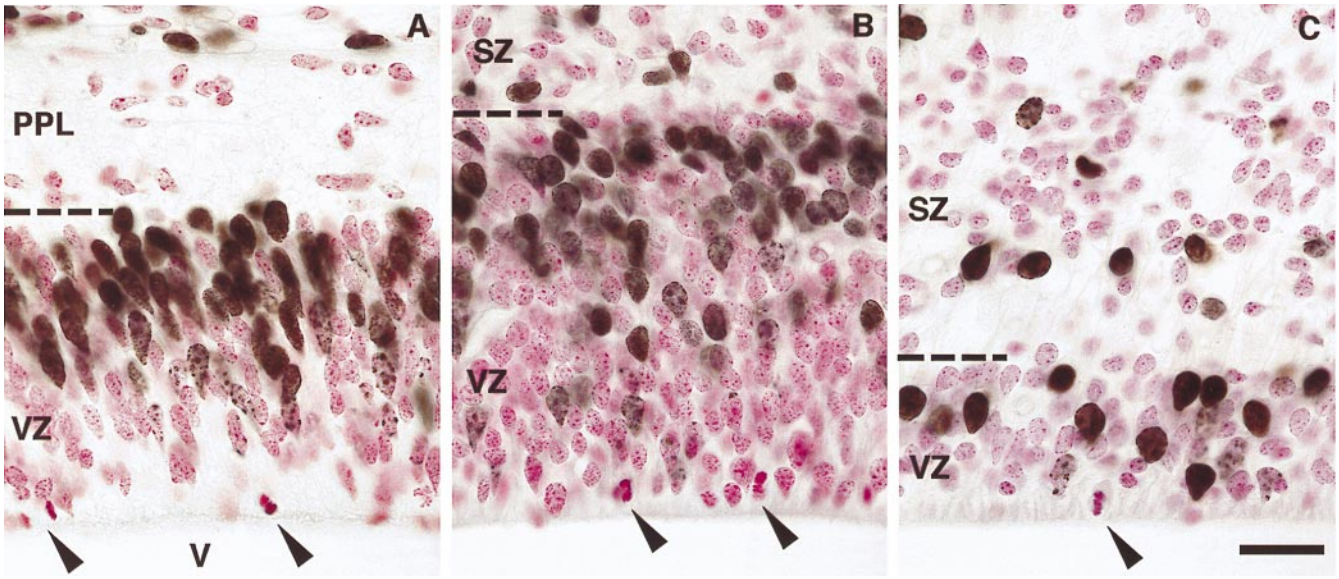

FIG. 1. The VZ of the medial occipital cerebral wall at E40 (*A*), E60 (*B*), and E80 (*C*), 30 min after a single injection of BrdUrd. BrdUrd-labeled cell nuclei are darkly stained, unlabeled nuclei are counterstained red, and counterstained M-phase cells (arrowheads) occupy the ventricular surface. In *A* the BrdUrd-labeled cells above the primitive plexiform layer (PPL) are at the cortical surface and are probably meningeal cells; such cells are not pictured in *B* and *C* because of the subsequent growth of the cerebral wall. Note the changes in thickness of the VZ with age. SZ, subventricular zone; V, cerebral ventricle; dashed lines, VZ/PPL border (*A*) or VZ/SZ border (*B* and *C*). (Bar = 20 μm.)

shortened to 4.6 hr by E80 (Fig. 3). The values for Ts at E40 and E80 are remarkably similar to reported estimates of Ts during rodent neurogenesis, which range from approximately 3 to 5 hr in mice (15) and from 5 to 9 hr in rats (11, 13, 14). In contrast, the approximately 10-hr rise and fall in Ts between E40 and E80 in monkeys differs from the relatively modest fluctuations in Ts during neurogenesis in rodents. Nonetheless, this developmental modulation of Ts in monkeys cannot account for the majority of the 40-hr difference in total cell cycle length between monkeys at E60 and rodents at a comparable stage. Thus, although total cell-cycle lengths vary greatly between monkeys and rodents, Ts is relatively conserved. This implies that the cell cycle is longer in monkeys than in rodents because of a lengthening of at least one cell-cycle phase other than S. This modification of phase length between species may indicate differences in mechanisms that regulate the timing of individual phases within the cycle (26–28).

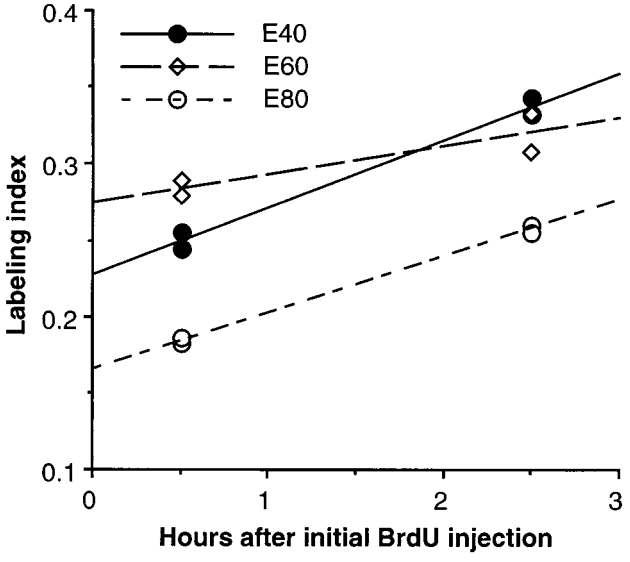

FIG. 2. Changes in LIs of monkey VZ with cumulative BrdUrd labeling at E40, E60, and E80. For each age, each survival time point (0.5 and 2.5 hr) is represented by two fetuses from two different mothers. Each data point is the mean LI of four nonconsecutive sections from a single brain. The SEM (not shown) of the mean LI of each brain is <8% at E40 and <5% at E60 and E80. [Note the closeness of the LI values (0.183 and 0.187) at E80 of the two fetuses at t = 0.5 hr, and of the two fetuses at t = 2.5 hr (0.256 and 0.260).]

DISCUSSION

This analysis provides the determination of cell-cycle and S-phase length in the developing nervous system of a primate species. Analysis of cumulative LIs indicated that cell-cycle duration in monkeys is substantially longer and follows a

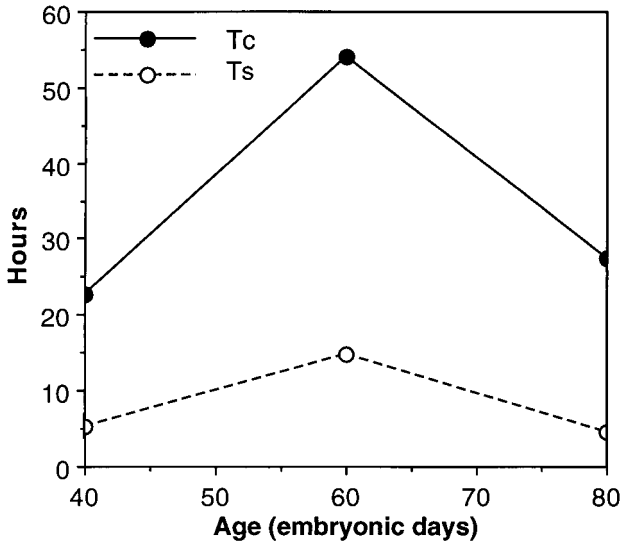

FIG. 3. Developmental profile of the lengths of the cell cycle (Tc) and S phase (Ts) during cortical neurogenesis in monkey VZ. The values of Tc and Ts at each age were calculated from the slope and y intercept, respectively, of the least-squares regression lines in Fig. 2. The height of the open circles indicates Ts, and the distance between the open and filled circles at each age indicates the combined lengths of G_1, G_2, and M.

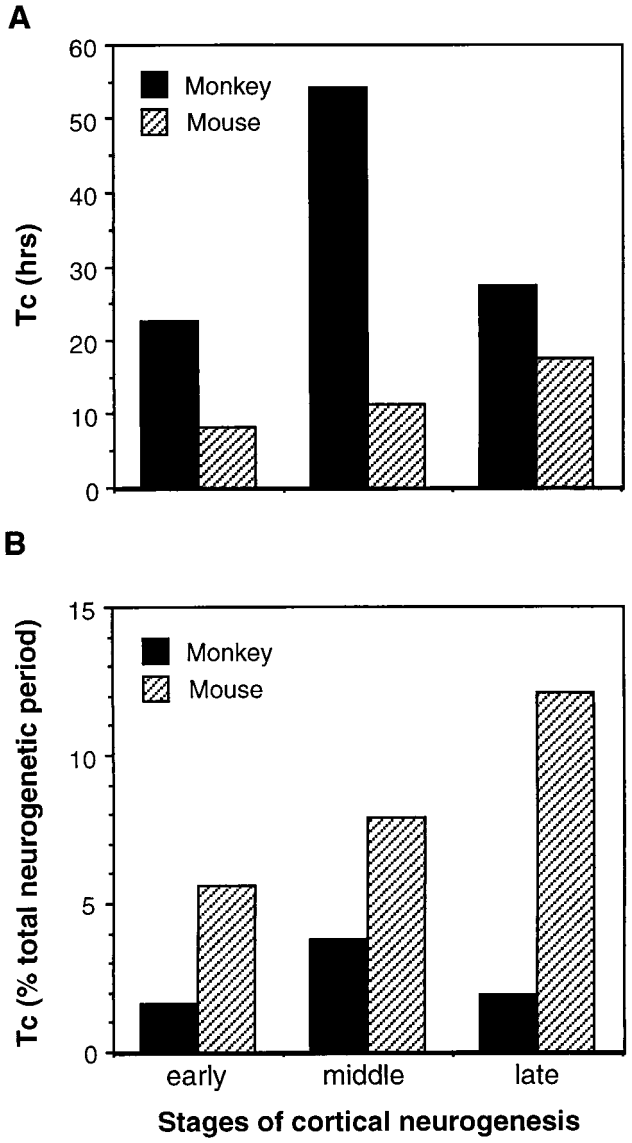

FIG. 4. Comparison of the length of the cell cycle (Tc) between monkey and mouse during cortical neurogenesis. Tc is compared at the beginning of the first (early), middle, and last (late) third of the total period of neurogenesis, corresponding to E40, E60, and E80 in monkeys and E11, E13, and E15 in mice. These three stages correlate respectively to the onset of neurogenesis for layer VI, the end of layer VI/onset of layer V neurogenesis, and the end of layer IV/onset of layer III neurogenesis (8, 9). (*A*) Tc expressed in absolute time. (*B*) Tc expressed as a proportion of the duration of the total neurogenetic period, which is 60 days in monkeys and 6 days in mice. Data for mice are from ref. 15.

different developmental course than in rodents, the only other mammals in which cell-cycle length has been measured during cortical neurogenesis.

The longer cell-cycle duration in monkeys compared with rodents might seem surprising, considering the increased number of neurons that must be produced during neurogenesis of the larger primate neocortex. However, given that the period of neurogenesis is 10-fold longer in monkeys than in rodents, a single cell cycle in the primate VZ actually constitutes a smaller fraction of the total neurogenetic period (Fig. 4*B*). Specifically, from our estimates of Tc we calculate that, depending on the developmental stage, the length of a single cell cycle in monkeys takes up only 1.6% to 3.8% of the 60-day period of neurogenesis. In contrast, cell-cycle lengths in mice constitute 6–13% of a 6-day neurogenetic period (from data in ref. 15) (Fig. 4*B*). This species difference implies that despite the longer cell cycles, substantially *more* successive rounds of cell division elapse during the neurogenetic period in monkeys than in rodents. In mice, it has been estimated that the total neurogenetic period is composed of 11 successive rounds of mitosis (15). In monkeys, if Tc increases linearly from 23 hr at E40 to 54 hr at E60, then descends linearly to 27 hr by E80, then approximately 28 rounds of cell division elapse from E40 to E80, which is substantially more than occur in mice. Examined in more detail, about 15 cell cycles would elapse from E40 to E60 in monkeys, compared with 5 cycles during the equivalent stage in mice (E11 to E13); and continuing, about 13 cycles would elapse between E60 and E80, compared with 3 cycles from E13 to E15 in mice. The implication of "extra" rounds of division in monkeys indicates that cell-cycle kinetics have been modified during primate evolution in a direction that would generate a greater number of cortical cells, and hence a larger neocortex.

Because, during mammalian cortical neurogenesis, cell divisions generate additional progenitors as well as postmitotic neurons (29–33), it is important to consider how the increased number of cell divisions in the primate VZ could contribute to cortical growth and histogenesis. Cell divisions that produce only progenitor "daughter" cells result in exponential expansion of the progenitor pool; in contrast, divisions that produce postmitotic neurons contribute directly to a particular developing cortical layer (29). Evidence from studies in mice indicates that early in neurogenesis (i.e., during the generation of neurons for deep layers VI and V), a round of cell division in the proliferative population produces substantially more progenitors than postmitotic neurons. As neurogenesis continues, this ratio gradually reverses, as each successive mitotic round generates increasingly greater proportions of neurons to progenitor cells, ultimately diminishing the progenitor pool (30, 34). This cytogenetic trend also appears to occur in ferrets (35), which belong to the order Carnivora, raising the possibility that this is a general feature of mammalian cortical development. If such a trend occurs in primates, which is consistent with the developmental changes in VZ thickness (Fig. 1), then increasing the number of successive cell divisions would be expected to have different effects on cortical growth as neurogenesis proceeds. Early on, "extra" rounds of division would contribute predominantly to progenitor cell production, causing a much greater increase in the size of the progenitor pool than in neuronal output to deep layers. As development continues and neuronal production eventually supplants progenitor production, "extra" rounds of division would cause a greater increase in neuronal output to the developing cortical layers than at earlier stages. In mice, the stage at which progenitor production equals that of postmitotic cells is attained during layer IV neurogenesis (30). Accordingly, a given "unit" of the VZ cell population in monkeys would be expected to produce more neurons for superficial cortical layers than would that of rodents.

This hypothesis can explain the expansive tangential growth of the primate cerebral VZ that occurs in early cortical neurogenesis (unpublished observation) and that ultimately forms the proliferative foundation for the enlarged cortical surface area of primates (29, 36). Moreover, this scenario may explain the development of species differences in the number and distribution of neurons among different cortical layers. A given column of primary visual cortex in primates contains approximately 2.5 times more neurons than that in rodents or other mammals; these additional neurons are concentrated mostly in the superficial layers (IV and II/III) (19, 37). This distribution, and the early expansion of the primate VZ, are consistent with our proposal that the "extra" cell divisions during early, deep layer neurogenesis in the primate contribute more toward increased progenitor than neuronal production, whereas those elapsing later (i.e., during superficial layer

neurogenesis) directly contribute more toward increased neuronal production. This hypothesis is in accord with studies indicating that laminar fate of cortical cells is determined at the level of dividing progenitor cells in the VZ (38, 39). Conceivably, evolutionary modification of other developmental processes, such as differential programmed cell death (40, 41), might also contribute to the formation of laminar variations in neuron number across species.

This hypothesis is consistent with the known hypercellularity of the superficial layers in the primary visual cortex of primates. However, other cortical areas in primates appear to have fewer superficial-layer neurons per columnar unit (19, 37), raising the possibility that proliferation parameters may vary regionally in the primate VZ. This is supported by evidence from [^{3}H]thymidine "birthdating" of cortical neurons in fetal rhesus monkeys, which shows that extrastriate cortex, which is adjacent to primary visual (striate) cortex and has fewer superficial layer neurons, has a shorter period of neurogenesis (42). Moreover, a comparison of LIs after single [^{3}H]thymidine injections in fetal macaque monkeys suggested that the rate of cell production is higher for primary visual cortex than for the adjacent extrastriate cortex during the period of superficial layer formation, and thus contributes to the additional superficial-layer neurons in striate versus extrastriate cortex (43). This suggests that cell-cycle kinetics may indeed vary regionally in the primate VZ during superficial layer formation, contributing to cytoarchitectonic differences among prospective overlying cortical areas.

While the relative schedule and sequence of neurogenesis for neocortical layers appear to be evolutionarily conserved (30), our findings indicate that the length, developmental course, and number of successive cell divisions constituting the neurogenetic period have been considerably modified since the time that rodents and primates last shared a common ancestor more than 70 million years ago (44). This implies that although both cell-cycle kinetics and the schedule of laminar formation are determined at the level of VZ progenitor cells, they are nonetheless regulated by distinct mechanisms and are evolutionarily dissociable. Indeed, *in vitro* studies have shown that proliferation and differentiation of cortical progenitor cells can be distinctly regulated by specific extracellular signaling molecules (45–47). This temporal dissociation of proliferation dynamics from laminar fate determination during evolution has provided an essential step leading toward neocortical enlargement in primates.

We thank Drs. R. S. Nowakowski and T. Takahashi for advice in carrying out this study, and our reviewers for their constructive comments on the manuscript. This work was supported by the U.S. Public Health Service.

1. Passingham, R. E. (1981) *Symp. Zool. Soc. London* **46,** 361–388.
2. Dunbar, R. I. M. (1992) *J. Hum. Evol.* **20,** 469–493.
3. Kaas, J. H. (1995) *Brain Behav. Evol.* **46,** 187–196.
4. Barton, R. A. (1996) *Proc. R. Soc. London Ser. B* **263,** 173–177.
5. Tomasello, M. & Call, J. (1997) *Primate Cognition* (Oxford Univ. Press, New York).
6. Blinkov, S. M. & Glezer, I. I. (1968) *The Human Brain in Figures and Tables: A Quantitative Handbook* (Plenum, New York).
7. Angevine, J. B. & Sidman, R. L. (1961) *Nature (London)* **192,** 766–768.
8. Rakic, P. (1974) *Science* **183,** 425–427.
9. Caviness, V. S., Jr. (1982) *Dev. Brain Res.* **4,** 293–302.
10. Luskin, M. B. & Shatz, C. J. (1985) *J. Comp. Neurol.* **242,** 611–631.
11. Waechter, R. V. & Jaensch, B. (1972) *Brain Res.* **46,** 235–250.
12. Schmahl, W. (1983) *Anat. Embryol.* **167,** 355–364.
13. Miller, M. W. & Nowakowski, R. S. (1991) *Alcohol Clin. Exp. Res.* **15,** 229–232.
14. Reznikov, K. & van der Kooy, D. (1995) *J. Comp. Neurol.* **360,** 536–554.
15. Takahashi, T., Nowakowski, R. S. & Caviness, V. S., Jr. (1995) *J. Neurosci.* **15,** 6046–6057.
16. Hoffman, M. A. (1985) *J. Theor. Biol.* **112,** 77–95.
17. Nowakowski, R. S., Lewin, S. B. & Miller, M. W. (1989) *J. Neurocytol.* **18,** 311–318.
18. Rakic, P. (1990) in *The Principles of Design and Operation of the Brain* , eds. Eccles, J. C. & Creutzfeldt, O. (Springer, New York), pp. 25–48.
19. Peters, A. (1987) in *Further Aspects of Cortical Function, Including Hippocampus*, Cerebral Cortex, eds. Jones, E. G. & Peters, A. (Plenum, New York), Vol. 6, pp. 267–294.
20. Miller, M. W. (1992) *Brain Res.* **595,** 17–24.
21. Takahashi, T., Nowakowski, R. S. & Caviness, V. S., Jr. (1992) *J. Neurocytol.* **21,** 185–197.
22. Takahashi, T., Nowakowski, R. S. & Caviness, V. S., Jr. (1993) *J. Neurosci.* **13,** 820–833.
23. Cai, L., Hayes, N. L. & Nowakowski, R. S. (1997) *J. Neurosci.* **17,** 2079–2087.
24. Sidman, R. L., Miale, I. L. & Feder, N. (1959) *Exp. Neurol.* **1,** 322–333.
25. Raedler, E., Raedler, A. & Feldhaus, S. (1980) *Anat. Embryol.* **158,** 253–269.
26. Ohtsubo, M., Theodoras, A. M., Schumacher, J., Roberts, J. M. & Pagano, M. (1995) *Mol. Cell. Biol.* **15,** 2612–2624.
27. Edger, B. A. & Lehner, C. F. (1996) *Science* **274,** 1646–1652.
28. Wuarin, J. & Nurse, P. (1996) *Cell* **85,** 785–787.
29. Rakic, P. (1988) *Science* **241,** 170–176.
30. Caviness, V. S., Jr., Takahashi, T. & Nowakowski, R. S. (1995) *Trends Neurosci.* **18,** 379–383.
31. Kornack, D. R. & Rakic, P. (1995) *Neuron* **15,** 311–321.
32. Cai, L., Hayes, N. L. & Nowakowski, R. S. (1997) *J. Neurosci.* **17,** 2088–2100.
33. Mione, M. C., Cavanagh, J. F. R., Harris, B. & Parnavelas, J. G. (1997) *J. Neurosci.* **17,** 2018–2029.
34. Takahashi, T., Nowakowski, R. S. & Caviness Jr., V. S. (1996) *J. Neurosci.* **16,** 6183–6196.
35. Chenn, A. & McConnell, S. K. (1995) *Cell* **82,** 631–641.
36. Rakic, P. (1995) *Trends Neurosci.* **18,** 383–388.
37. Rockel, A. J., Hiorns, R. W. & Powell, T. P. S. (1980) *Brain* **103,** 221–244.
38. McConnell, S. K. & Kaznowski, C. E. (1991) *Science* **254,** 282–285.
39. Frantz, G. D. & McConnell, S. K. (1996) *Neuron* **17,** 55–61.
40. Ferrer, I., Soriano, E., Del Rio, J. A., Alcántara, S. & Auladell, C. (1992) *Prog. Neurobiol.* **39,** 1–43.
41. Finlay, B. L. (1992) *J. Neurobiol.* **23,** 1159–1171.
42. Rakic, P. (1976) *Exp. Brain Res. Suppl.* **1,** 244–248.
43. Dehay, C., Giroud, P., Berland, M., Smart, I. & Kennedy, H. (1993) *Nature (London)* **366,** 464–466.
44. Novacek, M. J. (1992) *Nature (London)* **356,** 121–125.
45. Ghosh, A. & Greenberg, M. E. (1995) *Neuron* **15,** 89–103.
46. Vicario-Abejón, C., Johe, K. K., Hazel, T. G., Collazo, D. & McKay, R. D. G. (1995) *Neuron* **15,** 105–114.
47. Lu, N. & DiCicco-Bloom, E. (1997) *Proc. Natl. Acad. Sci. USA* **94,** 3357–3362.